

Supporting Information

From $[B_6O_{13}]^{8-}$ to $[GaB_5O_{13}]^{8-}$ to $[Ga\{B_5O_9(OH)\}\{BO(OH)_2\}]^{2-}$:

Synthesis, structure and nonlinear optical property of the new metal borates

Qi-Ming Qiu and Guo-Yu Yang*

MOE Key Laboratory of Cluster Science, School of Chemistry and Chemical Engineering, Beijing Institute of Technology, Beijing 100081, China. E-mail: ygy@bit.edu.cn, Fax: (+86)10-6891-8572

Table of Contents

Table S1 Selected bond distances (Å) and angles (°) for 1	1
Table S2 Selected bond distances (Å) and angles (°) for 2	1
Table S3 Selected bond distances (Å) and angles (°) for 3	2
Table S4 Selected H-bonding distances (Å) and angles (°) for 1	3
Table S5 Selected H-bonding distances (Å) and angles (°) for 2	3
Table S6 Selected H-bonding distances (Å) and angles (°) for 3	3
Fig. S1 View of cubic cavity, topology network and stacking structures of 1	4
Fig. S2 View of the 9-MR channels along the <i>b</i> axis in 2	4
Fig. S3 Structure comparisons between 2 and 2a	5
Fig. S4 The asymmetric unit and 1D chain of $[Ga(en)_2][B_5O_8(OH)_2]\cdot H_2O$ (3a)	5
Fig. S5 PXRD patterns show the comparison between the experimental value and calculated ones for compounds 1(a) , 2(b) and 3(c)	6
Fig. S6 TG curves for compounds 1(a) , 2(b) and 3(c)	7
Fig. S7 IR spectra for compounds 1(a) , 2(b) and 3(c)	8
Fig. S8 UV/Vis diffuse reflectance spectra of compounds 1(a) , 2(b) and 3(c)	9
Fig. S9 Oscilloscope traces of SHG signals for compound 2 and $LiNbO_3$	9

Table S1 Selected bond distances (\AA) and angles ($^\circ$) for **1**

O2—K ⁱⁱ	3.346 (2)	O2—B2 ⁱ	1.453 (2)
K—O1 ^{iv}	2.7906 (14)	O1—B1	1.358 (2)
K—O1 ^v	2.7906 (14)	O1—B2	1.4457 (19)
K—O1	2.7906 (14)	O3—B1	1.3632 (19)
K—O1 ^{vi}	2.9148 (15)	O3—B2 ^{vii}	1.457 (2)
K—O1 ^{viii}	2.9148 (15)	O4—B2 ⁱ	1.5304 (16)
K—O1 ⁱⁱⁱ	2.9148 (15)	O4—B2 ^{viii}	1.5304 (16)
K—O5	3.113 (3)	O4—B2	1.5304 (16)
		O2—B1	1.377 (2)

Symmetry codes: (i) y, z, x ; (ii) $-x + 1, y - 1/2, -z + 1/2$; (iii) $-x + 1, -y + 1, -z$; (iv) $-y + 1, z + 1/2, -x + 1/2$; (v) $-z + 1/2, -x + 1, y - 1/2$; (vi) $y, -z + 1/2, x - 1/2$; (vii) $z + 1/2, x, -y + 1/2$; (viii) z, x, y .

Table S2 Selected bond distances (\AA) and angles ($^\circ$) for **2**

Ga—O1	1.795 (10)	O1—B1	1.359 (19)
Ga—O6 ⁱⁱ	1.801 (10)	O3—B1	1.39 (2)
Ga—O10 ⁱⁱⁱ	1.832 (9)	O3—B2	1.41 (2)
Ga—O8 ^{iv}	1.834 (9)	O5—B3	1.390 (18)
B5—O9 ⁱ	1.432 (17)	B4—O9	1.358 (18)
B5—O5	1.47 (2)	O7—B4	1.363 (18)
B5—O2	1.48 (2)	B3—O4	1.367 (18)
B5—O10	1.507 (16)	B2—O4	1.482 (19)
O8—B4	1.358 (17)	O7—B2	1.460 (17)
O10—B2	1.550 (17)	N2—C1	1.46 (2)
O6—B3	1.316 (19)	C2—C1	1.47 (2)
O2—B1	1.348 (18)	N1—C2	1.493 (19)
N2—C1	1.46 (2)	C2—C1	1.47 (2)

Symmetry codes: (i) $x + 1, y, z$; (ii) $x, y + 1, z$; (iii) $x, -y + 1, z + 1/2$; (iv) $x + 1, -y + 1, z + 1/2$.

Table S3 Selected bond distances (\AA) and angles ($^\circ$) for **3**

Cs—O8 ⁱ	2.997 (4)	O3—B1	1.357 (7)
Cs—O4	3.013 (4)	O3—B3	1.485 (7)
Cs—O13 ⁱⁱ	3.137 (4)	O2—B1	1.364 (7)
Cs—O10 ⁱⁱⁱ	3.173 (4)	O2—B2	1.381 (7)
Cs—O12 ⁱ	3.340 (5)	O9—B5	1.387 (7)
Cs—O11 ^{iv}	3.454 (4)	O9—B4	1.406 (6)
Cs—O2	3.457 (4)	O5—B2	1.376 (7)
Cs—O9 ⁱ	3.530 (4)	O5—B3	1.444 (6)
Ga—O11	1.803 (4)	O11—B6	1.340 (7)
Ga—O8 ^v	1.806 (4)	O6—B4	1.357 (7)
Ga—O10	1.813 (4)	O6—B3	1.470 (7)
Ga—O4 ^{iv}	1.822 (4)	O4—B2	1.332 (6)
Na—O1 ⁱⁱⁱ	2.333 (4)	O7—B5	1.352 (7)
Na—O10	2.383 (4)	O7—B3	1.469 (7)
Na—O5 ^{iv}	2.424 (4)	O8—B4	1.342 (7)
Na—O6 ^v	2.555 (4)	O13—B6	1.371 (7)
Na—O7	2.671 (4)	O10—B5	1.362 (7)
Na—O5 ^v	2.871 (4)	O12—B6	1.370 (7)
Na—O7 ^{iv}	2.981 (4)	O1—B1	1.387 (7)

Symmetry codes: (i) $x, y - 1, z - 1$; (ii) $x - 1, y - 1, z - 1$; (iii) $-x + 1, -y, -z + 1$; (iv) $-x + 1, -y + 1, -z + 1$; (v) $x + 1, y, z$.

Table S4 Selected H-bonding distances (\AA) and angles ($^\circ$) for **1**

D–H	d(D–H)	d(H···A)	\angle DHA	d(D···A)	A	Symmetry
O7–H7	0.78	1.80	117	2.226	O7	[$-x + 1, -y, -z + 2$]
O5–H5A	0.87	1.74	124	2.338	O2	[$-x + 1, y + 1/2, -z + 1/2$]
O5–H5B	0.86	1.78	121	2.338	O2	[$-y + 1/2, -z + 1, x - 1/2$]
O5–H5A	0.87	1.53	146	2.299	O3	[$-x + 1, y + 1/2, -z + 1/2$]
O5–H5B	0.86	1.54	145	2.299	O3	[$-y + 1/2, -z + 1, x - 1/2$]
O6–H6	0.85	2.47	158	3.265	O1	[$y, -z + 1/2, x + 1/2$]

Table S5 Selected H-bonding distances (\AA) and angles ($^\circ$) for **2**

D–H	d(D–H)	d(H···A)	\angle DHA	d(D···A)	A	Symmetry
N1–H1E	0.89	2.39	175	3.275	O7	[$x, -y, z + 1/2$]
N1–H1D	0.89	1.81	174	2.693	O4	
N1–H1C	0.89	1.85	168	2.724	O5	[$x - 1, y, z$]
N2–H2E	0.89	2.27	163	3.134	O9	[$x, -y + 1, z + 1/2$]
N2–H2D	0.89	2.04	160	2.890	O1	[$x, -y + 1, z + 1/2$]
N2–H2C	0.89	1.97	151	2.782	O8	[$x, y, z + 1$]

Table S6 Selected H-bonding distances (\AA) and angles ($^\circ$) for **3**

D–H	d(D–H)	d(H···A)	\angle DHA	d(D···A)	A	Symmetry
O13–H13	0.82	1.94	176	2.761	O3	[$-x + 1, -y + 1, -z + 2$]
O12–H12	0.82	2.45	129	3.035	O9	[$-x + 1, -y + 2, -z + 2$]
O12–H12	0.82	2.41	127	2.974	O11	[$-x + 1, -y + 2, -z + 2$]
O1–H1	0.82	1.97	163	2.766	O12	[$-x + 1, -y + 1, -z + 2$]

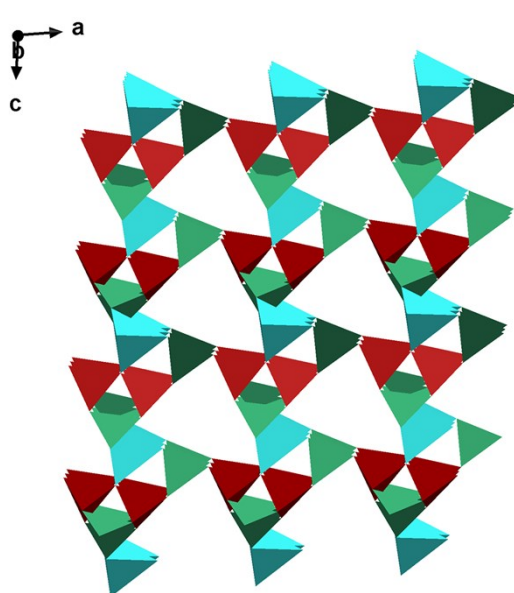
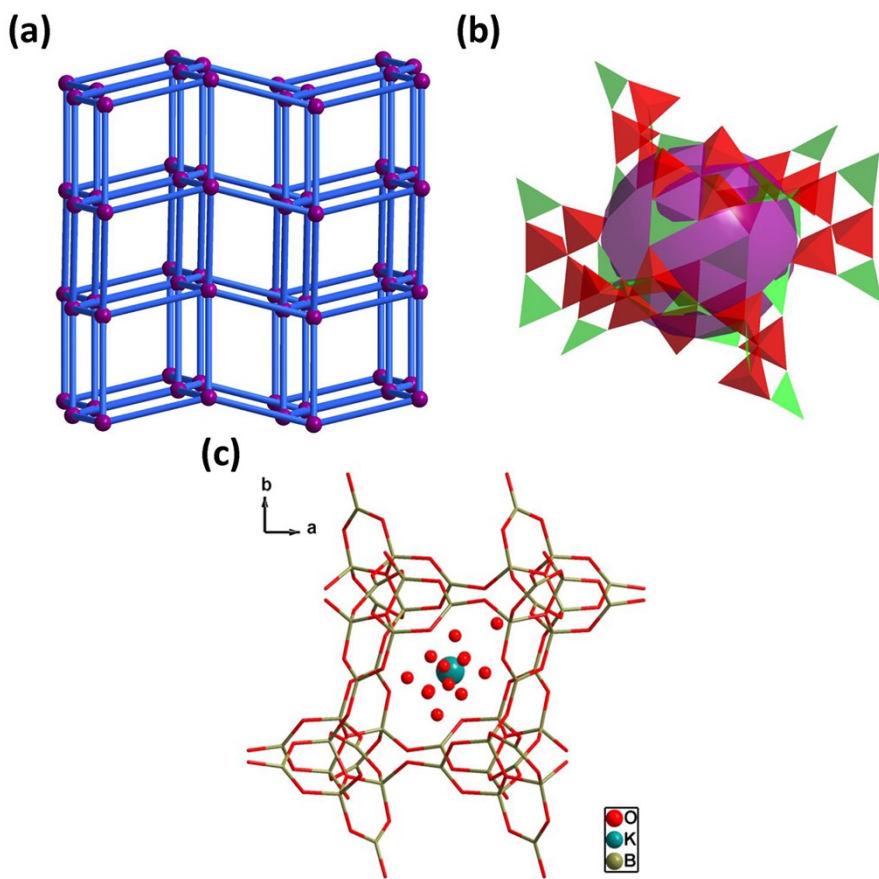


Fig. S2 View of the 9-MR channels along the *b* axis in **2**.

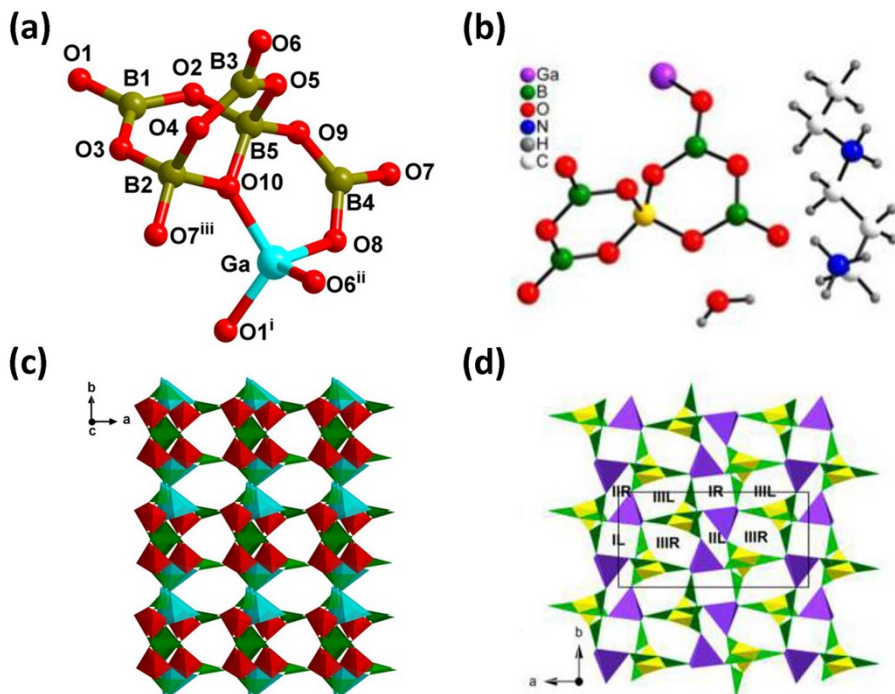


Fig. S3 (a) View of the structure of $[GaB_5O_{13}]^{8-}$ in compound **2**, symmetry codes: (i) $x, 1 - y, -0.5 + z$; (ii) $x, -y, -0.5 + z$; (iii) $1 + x, y, z$. (b) The asymmetric unit of **2a**. (c) View of the 9-MR channels along the c axis in **2**. (d) Polyhedral representation of the framework and three pairs of 8-MR channels along the c axis in **2a**.

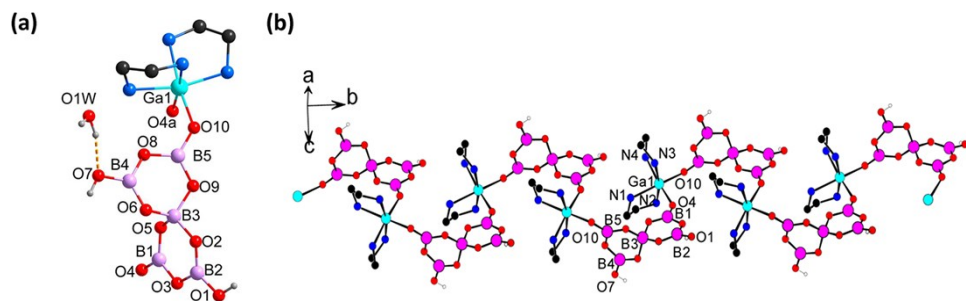


Fig. S4 (a) The asymmetric unit and (b) 1D chain of $[Ga(en)_2][B_5O_8(OH)_2] \cdot H_2O$ (**3a**). Cited from *Inorg. Chem.*, 2012, **51**, 8810–8817.

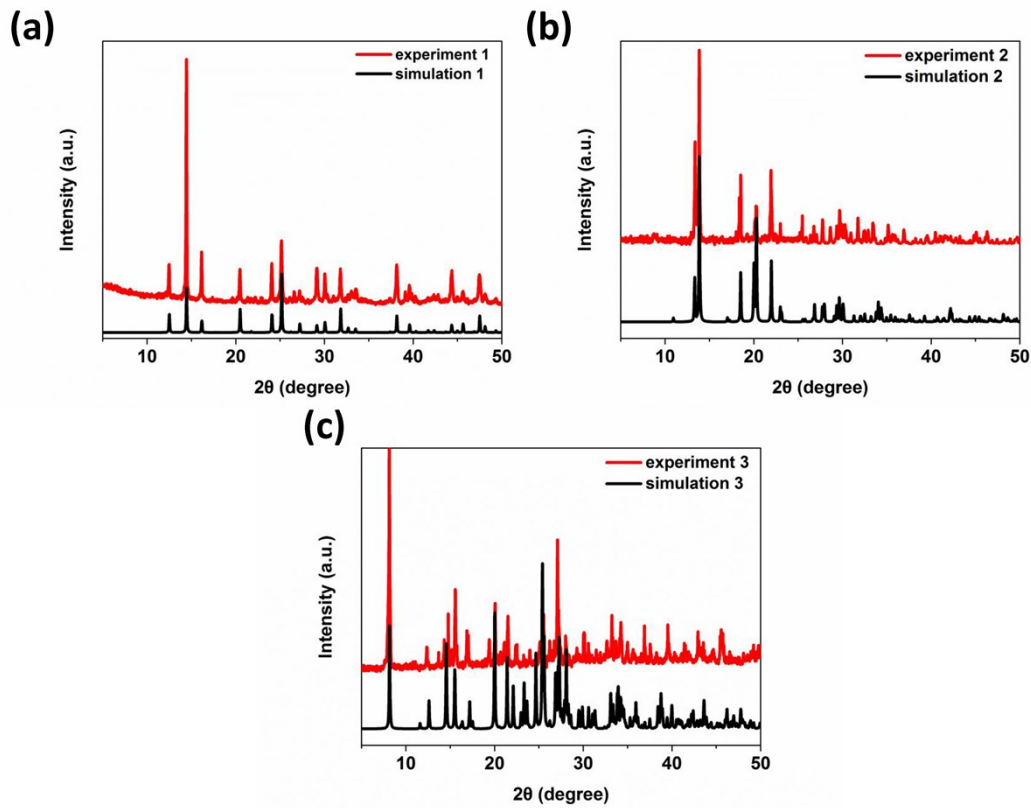


Fig. S5 PXRD patterns show the comparison between the experimental value and calculated ones for compounds 1(a), 2(b) and 3(c).

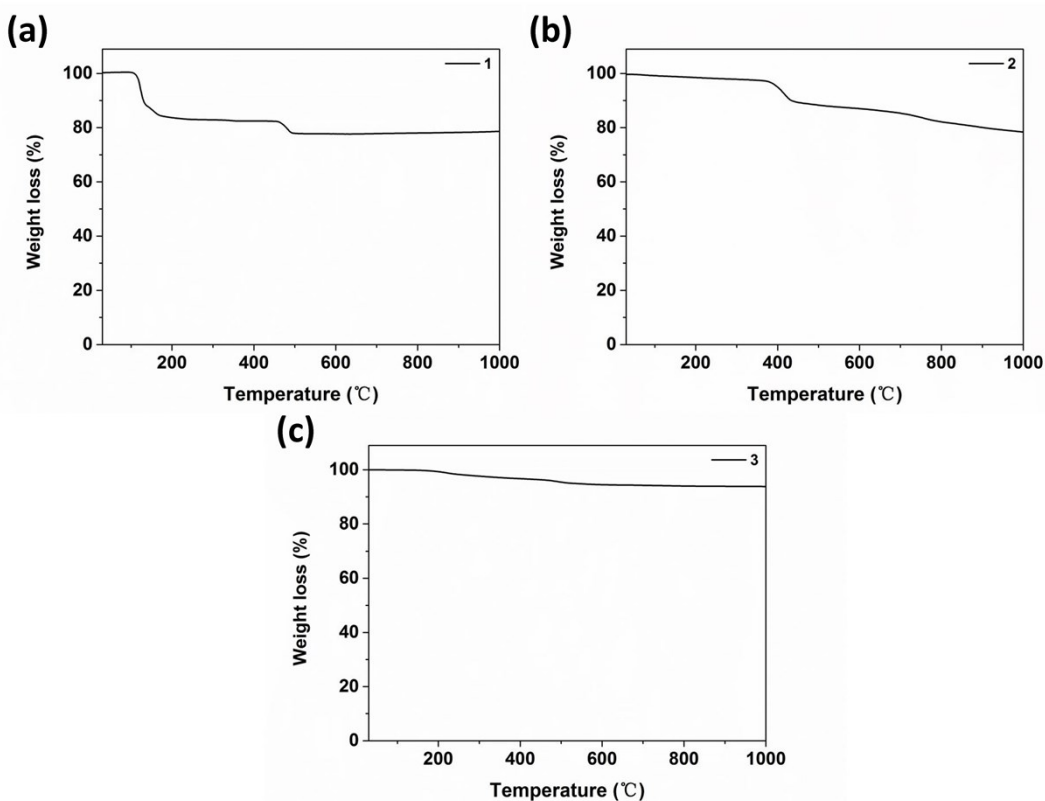


Fig. S6 TG curves for compounds **1(a)**, **2(b)** and **3(c)**.

The Thermogravimetric (TG) curves of compound **1–3** can be stable up to about 120, 380 and 180 °C, respectively. For **1**, the initial weight loss (obs. 15.8%, cal. 15.4%) in the temperature range 120–190°C is assigned to the loss of the water molecule. The second step ranging from 450–520°C corresponds to the dehydration of the hydrogen ion per formula unit (obs. 4.8%, cal. 4.7%). For **2**, the guest molecules were gradually lost from 380 to 800 °C (obs. 18.5%, cal. 17.9%). For **3**, the weight loss 6.4 % (cal. 5.4 %) in the temperature range 180–650°C is attributed to the removal of dehydration of the hydroxyls.

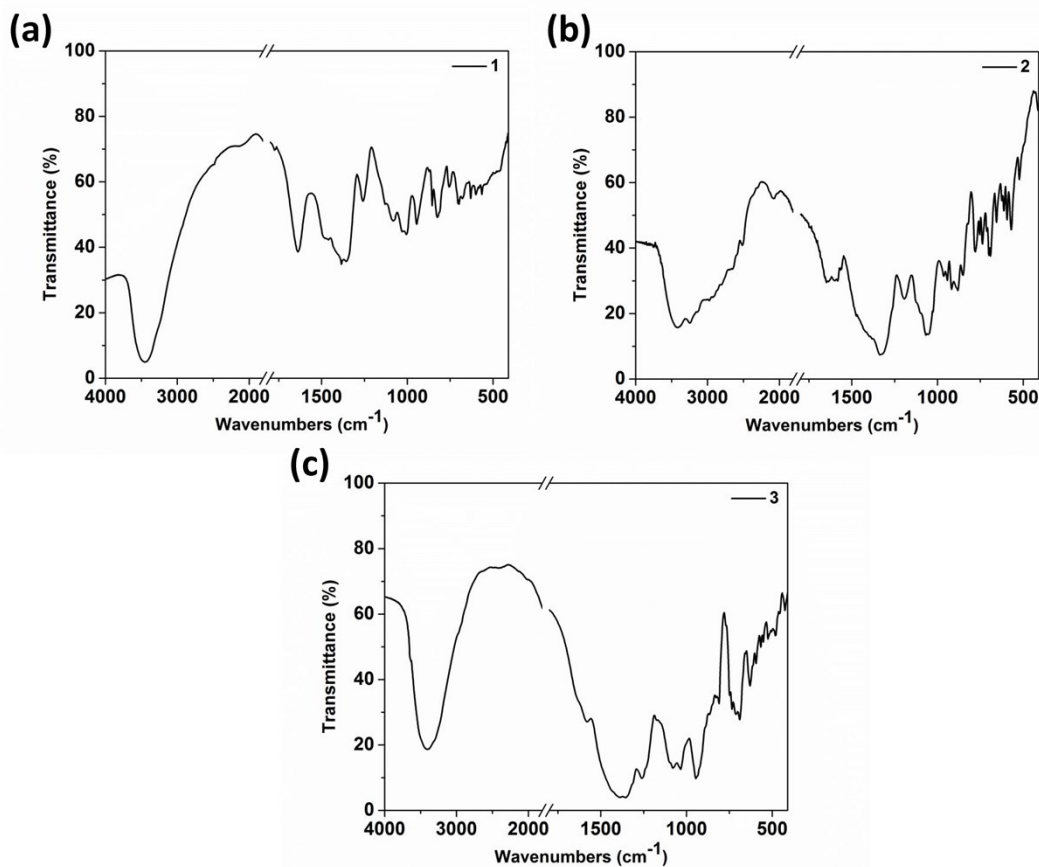


Fig. S7 IR spectra for compounds **1(a)**, **2(b)** and **3(c)**.

As for the IR spectra in **1–3**, the absorption bands around 3500–3000 cm^{-1} are related to vibrations of the O–H or N–H bonds. The stretching of BO_3 and BO_4 units are located at 1384–1334 cm^{-1} , 1260–1258 cm^{-1} , 963–945 cm^{-1} , 881–810 cm^{-1} , 698–689 cm^{-1} , respectively. The results of TGA and IR spectra are agreement with the single-crystal structures of **1–3**.

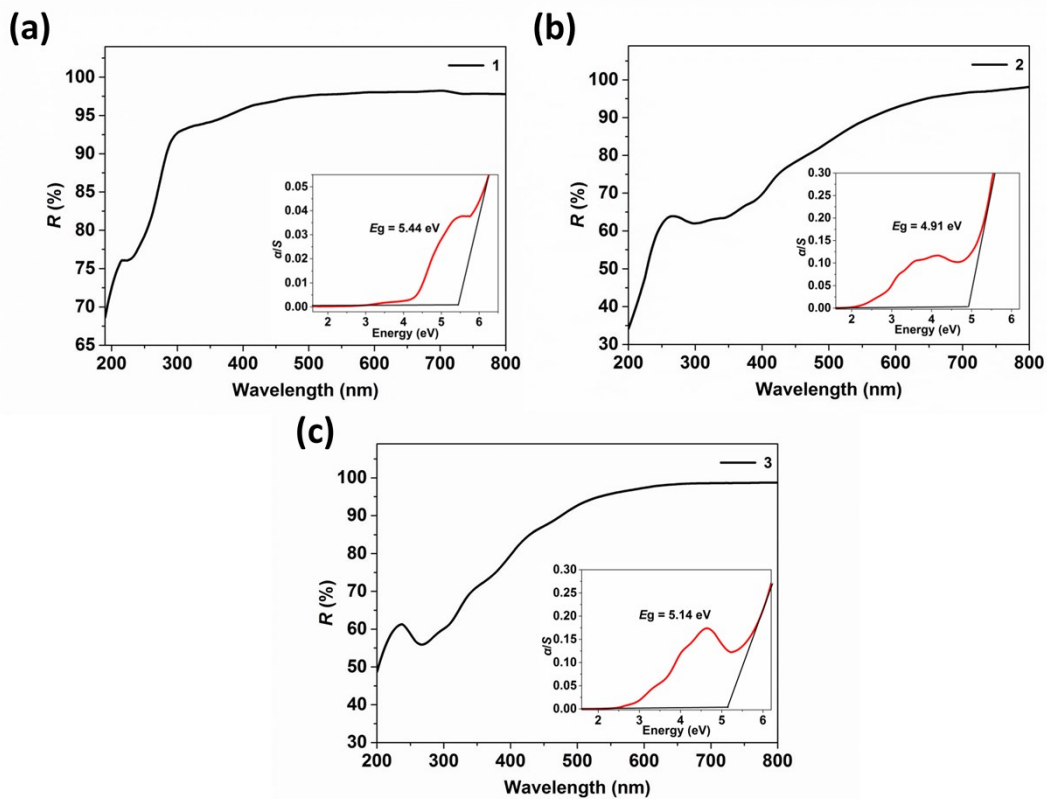


Fig. S8 UV/Vis diffuse reflectance spectra of compounds **1(a)**, **2(b)** and **3(c)**. Inset: plots of α/S vs. E .

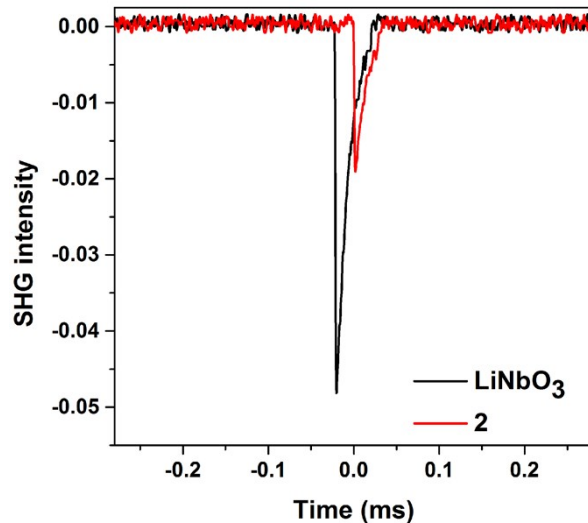


Fig. S9 Oscilloscope traces of SHG signals for compound **2** and LiNbO_3 in the same particle size of 150–212 μm .